A Gas-Kinetic BGK Solver for Two-Dimensional Turbulent Compressible Flow

Ong J. Chit, Ashraf A. Omar, Waqar Asrar and Ahmad F. Ismail
Department of Mechanical Engineering, International Islamic University Malaysia, Kuala Lumpur, Malaysia

Abstract - *In this paper, a gas kinetic solver is developed for the Reynolds Average Navier-Stokes (RANS) equations in two-space dimensions. To our best knowledge, this is the first attempt to extend the application of the BGK (Bhatnagaar-Gross-Krook) scheme to solve RANS equations with a turbulence model using finite difference method. The convection flux terms which appear on the left hand side of the RANS equations are discretized by a semi-discrete finite difference method. Then, the resulting inviscid flux functions are approximated by gas-kinetic BGK scheme which is based on the BGK model of the approximate collisional Boltzmann equation. The cell interface values required by the inviscid flux functions are reconstructed to higher-order spatial accuracy via the MUSCL (Monotone Upstream-Centered Schemes for Conservation Laws) variable interpolation method coupled with a minmod limiter. As for the diffusion flux terms, they are discretized by a second-order central difference scheme. To account for the turbulence effect, a combined k-ε / k-ω SST (Shear-Stress Transport) two-equation turbulence model is used in the solver. An explicit-type time integration method known as the modified fourth-order Runge-Kutta method is used to compute steady-state solutions. The computed results for a supersonic flow past a flat plate where the transition is artificially triggered at 50% of plate length are presented in this paper. Validating the computed results against existing analytical solutions and also comparing them with results from other well-known numerical schemes show that a very good agreement is obtained.*

Keywords: Finite Difference Method, BGK Scheme, Compressible Turbulent Flow, Turbulence Model.

1 Introduction

Throughout the history of computational fluid dynamics development, many numerical schemes have been created to solve practical application of gas dynamics. The key design criterion of any numerical schemes is to maximize robustness and accuracy. This requirement is particularly important in compressible flows involving high-speed flow where intense shock waves and boundary layers may simultaneously exist. Among those notable and successful are the Godunov-type and flux vector splitting schemes. Besides these numerical schemes that stem from the discretization of the convective terms, the gas-kinetic schemes have attracted much attention in recent years due to their high robustness and accuracy.

Recent developments have seen the emergence of another class of scheme known as the gas-kinetic schemes that are developed based on the Boltzmann equation. [15,19] Mainly, there are two groups of gas-kinetic schemes and the difference lies within the type of Boltzmann equation use in the gas evolution stage. One of them is the well-known KFVS (Kinetic Flux Vector Splitting) scheme which is based on the collisionless Boltzmann equation and the other is based on the collisional BGK (Bhatnagaar-Gross-Krook) model [3] where the BGK scheme is derived. Like any other FVS method, the KFVS scheme is very diffusive and less accurate in comparison with the Roe-type FDS method. The diffusivity of the FVS schemes is mainly due to the particle or wave-free transport mechanism, which sets the CFL time step equal to particle collision time. [4] In order to reduce diffusivity, particle collisions have to be modeled and implemented into the gas evolution stage. One of the distinct approaches to take particle collision into consideration in gas evolution can be found in Xu. [15] In this method, the collision effect is considered by the BGK model as an approximation of the collision integral in the Boltzmann equation. It is found that this gas-kinetic BGK scheme possesses accuracy that is superior to the flux vector splitting schemes and avoids the anomalies of FDS-type schemes. [5-9]

Turbulent flow motions occur in vast majority of fluid applications. To name a few: fluid flow in a pipe, flow processes in combustion chamber and even flow over an airfoil will exhibit a chaotic complex motion defined as turbulent flow. The most elegant solution to any turbulent flow is via the Direct Numerical Simulation (DNS) of turbulence. This approach is implemented by discretizing the Navier-Stokes equations with higher order accurate numerical scheme and solved using extremely fine grid mesh. An alternative approach to the DNS technique would be the adoption of Large Eddy Simulation (LES), which draws the advantages of the direct simulation of turbulence flows and the solution of the Reynolds averaged equations through closure assumptions. Although the popularity of DNS and LES have become noticeable [10-12] due to rapid development of high performance computing technology,

the general trend of computing turbulent flows still remain with the solution of Reynolds-Averaged Navier-Stokes (RANS) equations with the inclusion of Reynolds stresses into the original full Navier-Stokes equations. Resolving the turbulent flows via this means proved to be computationally cheaper. [13,14] The closure equations that provide the additional Reynolds stresses in the RANS equations are calculated from turbulence models.

In the present work, a flow solver based on the gas-kinetic BGK scheme is developed and tested. The BGK scheme is used to approximate the convective flux terms, while a second-order central scheme is used to discretize the diffusive flux terms of the RANS equations, coupled with a combined *k-ε / k-ω* SST two-equation turbulence model to provide the required Reynolds stresses to resolve the turbulent flow. The numerical solver is tested with a supersonic flow past a flat plate where a transition is artificially triggered at 50% of plate length in order to assess its computational capabilities. The computed results are compared with existing analytical solutions of Spalding and Chi [1] and also comparing them with results from other well-known numerical schemes show that a very good agreement is obtained.

2 Numerical methods

The two-dimensional normalized Reynolds-averaged Navier-Stokes equations in the computational space can be written in strong conservation form as

$$\frac{\partial \overline{W}}{\partial t}+\frac{\partial \overline{F}}{\partial \xi}+\frac{\partial \overline{G}}{\partial \eta}=\frac{\partial \overline{F}_v}{\partial \xi}+\frac{\partial \overline{G}_v}{\partial \eta} \tag{1}$$

where

$$\overline{W}=\frac{1}{J}\begin{bmatrix}\rho\\ \rho U\\ \rho V\\ \rho\varepsilon\end{bmatrix},$$

$$\overline{F}=\frac{1}{J}\begin{bmatrix}\xi_x(\rho U)+\xi_y(\rho V)\\ \xi_x(\rho U^2+p)+\xi_y(\rho UV)\\ \xi_x(\rho UV)+\xi_y(\rho V^2+p)\\ \xi_x(\rho\varepsilon U+pU)+\xi_y(\rho\varepsilon V+pV)\end{bmatrix},$$

$$\overline{G}=\frac{1}{J}\begin{bmatrix}\eta_x(\rho U)+\eta_y(\rho V)\\ \eta_x(\rho U^2+p)+\eta_y(\rho UV)\\ \eta_x(\rho UV)+\eta_y(\rho V^2+p)\\ \eta_x(\rho\varepsilon U+pU)+\eta_y(\rho\varepsilon V+pV)\end{bmatrix}$$

$$\overline{F}_v=\frac{1}{J}\begin{bmatrix}0\\ \xi_x\tau_{xx}+\xi_y\tau_{xy}\\ \xi_x\tau_{xy}+\xi_y\tau_{yy}\\ \xi_x(U\tau_{xx}+V\tau_{xy}-q_x)+\xi_y(U\tau_{xy}+V\tau_{yy}-q_y)\end{bmatrix},$$

$$\overline{G}_v=\frac{1}{J}\begin{bmatrix}0\\ \eta_x\tau_{xx}+\eta_y\tau_{xy}\\ \eta_x\tau_{xy}+\eta_y\tau_{yy}\\ \eta_x(U\tau_{xx}+V\tau_{xy}-q_x)+\eta_y(U\tau_{xy}+V\tau_{yy}-q_y)\end{bmatrix}$$

With ρ, U, V, p and ε are the macroscopic density, x-component of velocity, the y-component of velocity, the pressure and total energy, respectively. While, τ_{xx}, τ_{xy}, τ_{yy} are the shear stress terms and q_x, q_y are the heat conduction terms along the *x*- and *y*-directions, respectively. A detailed description about the viscous shear stresses appearing in the above equations can be found in Hoffmann and Chiang. [16]

From the perspective of RANS computation, the viscosity μ in the stress terms and the term (μ / Pr) in the heat conduction terms are modeled as

$$\begin{aligned}\mu &= \mu_l+\mu_t\\ \frac{\mu}{p_r} &= \left(\frac{\mu}{p_r}\right)_l+\left(\frac{\mu}{p_r}\right)_t\end{aligned} \tag{2}$$

where the subscripts *l* and *t* represent laminar and turbulent contributions, respectively. The parameter $(Pr)_t$ is called the turbulent Prandtl number and for air it is generally taken to be 0.9 for wall bounded flows. The closure model chosen to yield the turbulent viscosity μ_t that appears in the RANS equations is the combined *k-ε / k-ω* SST two-equation turbulence model which is given as

$$\frac{\partial}{\partial t}(\rho k)+\frac{\partial}{\partial x_j}(\rho u_j k)=\frac{\partial}{\partial x_j}\left[(\mu+\sigma_k\mu_t)\frac{\partial k}{\partial x_j}\right]+P_k-\beta^*\rho\omega k \tag{3}$$

$$\begin{aligned}\frac{\partial}{\partial t}(\rho\omega)+\frac{\partial}{\partial x_j}(\rho u_j\omega) &= \frac{\partial}{\partial x_j}\left[(\mu+\sigma_\omega\mu_t)\frac{\partial \omega}{\partial x_j}\right]\\ &\quad+2(1-F_1)\rho\sigma_{\omega 2}\frac{1}{\omega}\frac{\partial k}{\partial x_j}\frac{\partial \omega}{\partial x_j}\\ &\quad+\alpha\frac{\omega}{k}P_k-\beta\rho\omega^2\end{aligned} \tag{4}$$

where the production of turbulence P_k is defined as

$$P_k=\left[\mu_t\left(\frac{\partial u_i}{\partial x_j}+\frac{\partial u_j}{\partial x_i}-\frac{2}{3}\delta_{ij}\frac{\partial u_k}{\partial x_k}\right)-\frac{2}{3}\rho k\delta_{ij}\right]\frac{\partial u_i}{\partial x_j} \tag{5}$$

The closure constants used in the preceding equations are outlined clearly in Ref. [17].

A standard BGK scheme is based on the collisional Boltzmann equation and it is written in two dimensions as [15]

$$\frac{\partial f}{\partial t} + u\frac{\partial f}{\partial x} + v\frac{\partial f}{\partial y} = \frac{(g - f)}{\tau} \tag{6}$$

where f is the real particle distribution function and g is the equilibrium state approached by f within a collision time scale τ. Both f and g are functions of space x, y; time t; particle velocity u, v; and internal degrees of freedom ς. The equilibrium state g in the 2D BGK model is the Maxwell-Boltzmann distribution function and it has the following form

$$g = \rho\left(\frac{\lambda}{\pi}\right)^{(K+2)/2} e^{-\lambda\left[(u-U)^2+(v-V)^2+\varsigma^2\right]} \tag{7}$$

where λ is a function of density and pressure, $\lambda = \rho / 2p$. ς is a K dimensional vector which accounts for the internal degrees of freedom such as molecular rotation, translation and vibration. The dimensional vector, K is related to the specific heat ratios and the space dimension by the relation $K = (4 - 2\gamma) / (\gamma - 1)$, where for a diatomic gas $\gamma = 1.4$. The relations between the densities of mass ρ, momentum (ρU,ρV), and total energy ε with the distribution function f are derived from the following moment relation

$$\begin{pmatrix} \rho \\ \rho U \\ \rho V \\ \varepsilon \end{pmatrix} = \int f\,\Psi\, d\Xi \tag{8}$$

where $d\Xi = dudvd\varsigma$ is the volume element in the phase space while Ψ is the vector of moments given as

$$\Psi = \begin{pmatrix} 1 \\ u \\ v \\ \frac{1}{2}\left(u^2 + v^2 + \varsigma^2\right) \end{pmatrix} \tag{9}$$

With the moment relation defined in Eq. (8), a similar approach could be adopted in obtaining the numerical fluxes across cell interfaces and they are given as

$$\begin{aligned} F_x &= \int uf\,\Psi\, d\Xi \\ G_y &= \int vf\,\Psi\, d\Xi \end{aligned} \tag{10}$$

where F_x and G_y are the physical flux in the x- and y-direction, respectively. A general solution for f of Eq. (7) at the cell interface ($x_{i+1/2}$, y_j) in two-dimensions is obtained as [7]

$$f(0,0,t,u,v,\varsigma) = (1-\varphi)g_o + \varphi\, f_o(-ut,-vt) \tag{11}$$

where $\varphi = e^{-t/\tau}$ is an adaptive parameter. For a first-order scheme φ can be fixed in the numerical calculations. When the BGK scheme is extended to high-order, the value of φ should depend on the real flow situations. Finally, the gas-kinetic BGK numerical flux across the cell interface in the x-direction can be computed as

$$\begin{aligned} F_x &= \int u\, f(0,0,t,u,v,\varsigma)\,\Psi\, d\Xi \\ F_x &= (1-\varphi)F_x^e + \varphi\, F_x^f \end{aligned} \tag{12}$$

where F^e_x is the equilibrium flux function and F^f_x is the non-equilibrium or free stream flux function. Hence, the numerical flux for the BGK scheme at the cell interface in the x-direction are obtained from Eq. (12) as,

$$F_{i+1/2,j} = (1-\varphi)F^e_{i+1/2,j} + \varphi\, F^f_{i+1/2,j} \tag{13}$$

While the numerical flux at the cell interface in the y-direction is obtained in a similar manner and the resulting relation is presented as

$$G_{i,j+1/2} = (1-\varphi)G^e_{i,j+1/2} + \varphi\, G^f_{i,j+1/2} \tag{14}$$

In extending the numerical scheme to high-order spatial accuracy, the MUSCL approach [18] is adopted together with the minmod limiter. Hence, the left and right states of the primitive variables ρ, U, V, p at a cell interface could be obtained through the non-linear reconstruction of the respective variables and are given as

$$\begin{aligned} Q_l &= Q_{i,j} + \frac{1}{2}\phi\left(\frac{\Delta Q_{i+1/2,j}}{\Delta Q_{i-1/2,j}}\right)\Delta Q_{i-1/2,j} \\ Q_r &= Q_{i+1,j} - \frac{1}{2}\phi\left(\frac{\Delta Q_{i+3/2,j}}{\Delta Q_{i+1/2,j}}\right)\Delta Q_{i+1/2,j} \end{aligned} \tag{15}$$

where Q is a primitive variable and the subscript l, and r correspond to the left and right side of a considered cell interface. In addition, $\Delta Q_{i+1/2,j} = Q_{i+1,j} - Q_{i,j}$; $\Delta Q_{i-1/2,j} = Q_{i,j} - Q_{i-1,j}$; and $\Delta Q_{i+3/2,j} = Q_{i+2,j} - Q_{i+1,j}$. The minmod limiter used in the reconstruction of flow variables in Eq. (15) is given as

$$\phi(\Omega) = \min \mathrm{mod}(1,\Omega) = \max\left[0, \min(1,\Omega)\right] \tag{16}$$

Where the quantity Ω is determined based on the ratio of ($\Delta Q_{i+1/2,j}$ / $\Delta Q_{i-1/2,j}$) for left hand side reconstruction and ($\Delta Q_{i+3/2,j}$ / $\Delta Q_{i+1/2,j}$) for right hand side reconstruction, respectively.

For the time integration of steady state problems, an explicit formulation is chosen for the current solver which

utilizes a fourth-order Runge-Kutta method. Applying this method to the generalized two-dimensional RANS equations provides the following results

$$
\begin{aligned}
\overline{W}_{i,j}^{(1)} &= \overline{W}_{i,j}^{n} \\
\overline{W}_{i,j}^{(2)} &= \overline{W}_{i,j}^{n} - \frac{\Delta t}{4}\left[\left(\frac{\partial \overline{F}}{\partial \xi}\right)_{i,j}^{(1)} + \left(\frac{\partial \overline{G}}{\partial \eta}\right)_{i,j}^{(1)} - \left(\frac{\partial \overline{F}_v}{\partial \xi}\right)_{i,j}^{(1)} - \left(\frac{\partial \overline{G}_v}{\partial \eta}\right)_{i,j}^{(1)}\right] \\
\overline{W}_{i,j}^{(3)} &= \overline{W}_{i,j}^{n} - \frac{\Delta t}{3}\left[\left(\frac{\partial \overline{F}}{\partial \xi}\right)_{i,j}^{(2)} + \left(\frac{\partial \overline{G}}{\partial \eta}\right)_{i,j}^{(2)} - \left(\frac{\partial \overline{F}_v}{\partial \xi}\right)_{i,j}^{(2)} - \left(\frac{\partial \overline{G}_v}{\partial \eta}\right)_{i,j}^{(2)}\right] \\
\overline{W}_{i,j}^{(4)} &= \overline{W}_{i,j}^{n} - \frac{\Delta t}{2}\left[\left(\frac{\partial \overline{F}}{\partial \xi}\right)_{i,j}^{(3)} + \left(\frac{\partial \overline{G}}{\partial \eta}\right)_{i,j}^{(3)} - \left(\frac{\partial \overline{F}_v}{\partial \xi}\right)_{i,j}^{(3)} - \left(\frac{\partial \overline{G}_v}{\partial \eta}\right)_{i,j}^{(3)}\right] \\
\overline{W}_{i,j}^{n+1} &= \overline{W}_{i,j}^{n} - \Delta t\left[\left(\frac{\partial \overline{F}}{\partial \xi}\right)_{i,j}^{(4)} + \left(\frac{\partial \overline{G}}{\partial \eta}\right)_{i,j}^{(4)} - \left(\frac{\partial \overline{F}_v}{\partial \xi}\right)_{i,j}^{(4)} - \left(\frac{\partial \overline{G}_v}{\partial \eta}\right)_{i,j}^{(4)}\right]
\end{aligned}
\qquad (17)
$$

3 Results and discussions

3.1 Supersonic flow over flat plate

The objective of this test case is to provide a platform to validate the solutions obtained from the developed BGK flow solver incorporated with a turbulence model (i.e. combined *k-ε / k-ω* SST) with an existing analytical solution given by Spalding and Chi. [1]

In this flow problem, an incoming supersonic laminar flow is initiated in the free stream. The transition to turbulent flow along the flat plate is artificially triggered and placed at 50 % of the plate length. The following free stream conditions are specified: Mach number M_∞ = 2.0, density ρ = 1.25 kg/m^3, temperature T_∞ = 300.0 K and Reynolds number Re_∞ = 3.762x10^6. The Reynolds number is based on a reference length taken as L_∞ = 0.08 m. A structure grid is created by an algebraic grid generation method with clustering near the surface and at the inlet to resolve high flow gradient areas. The resulting mesh has a size of 100 by 50 grid points and is shown in Fig. 1. As for the specification of condition along the boundaries, the following are enforced: at left boundary the inflow conditions are specified as free-stream; at right and top boundaries, their conditions are determined by means of extrapolation from the interior domain; and the bottom boundary which locates the flat plate is set to assume adiabatic wall with no-slip conditions.

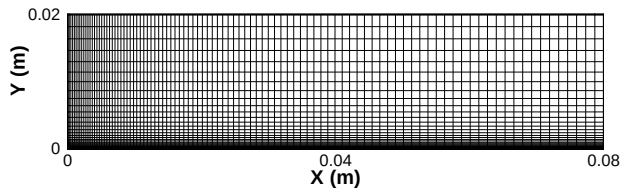

Figure 1: Computational domain for supersonic flow over a flat plate.

The quantities computed via the numerical solvers that are presented in this paper consist of skin friction coefficient, non-dimensional velocity profile (located at x = 0.06 m), and boundary layer thickness, presented in Fig. 2-4. Through these figures, comparisons are made among the numerical schemes themselves and to the analytical data that will provide a good ground to assess the computational behavior of each scheme with the circle symbol representing the analytical data. Figure 2 compares the skin friction coefficient distributions along the flat plate. The results depicted in this figure showed that the BGK scheme is capable of resolving the skin friction coefficient accurately prior to transition but with a small disagreement in the turbulent section of the flow where such a small percentage of disagreement in the prediction of turbulent flow has been reported to be acceptable.. This behavior is also evident in other numerical schemes' results such as Roe FDS scheme and central difference scheme with TVD.

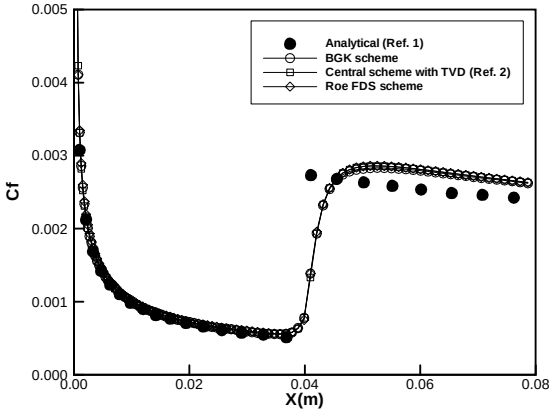

Figure 2: Comparisons of skin friction coefficients for the turbulent flat plate at M_∞= 2.0 and Re_∞ = 3.762E06.

Next, the comparisons of non-dimensional velocity profiles located at x = 0.06 m is presented in Fig. 3. The illustrated results in this figure showed that a good agreement can be seen among the numerical results with the analytical data.

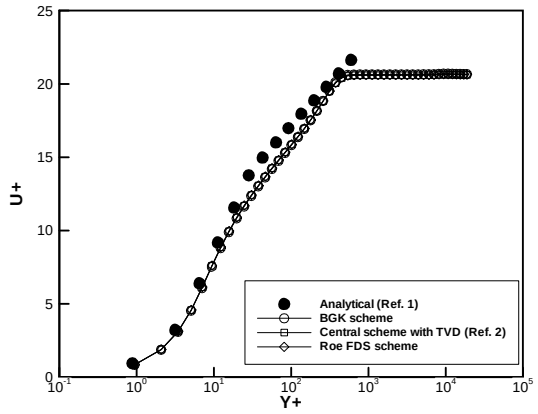

Figure 3: Comparison of velocity profiles for the turbulent flat plate at M∞= 2.0 and Re∞ = 3.762E06.

This deduction can also be applied and seen in Fig. 4 which illustrates the comparisons of boundary layer thickness generated by each numerical solver.

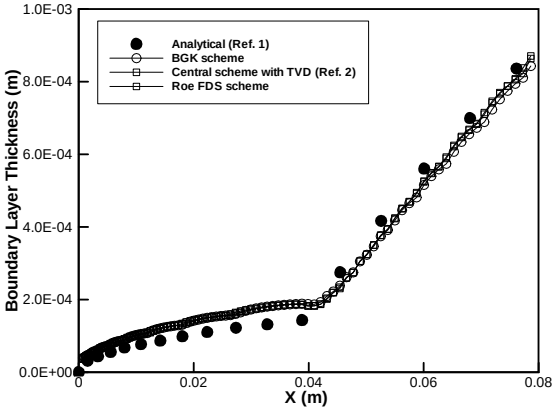

Figure 4: Comparison of boundary layer thicknesses for the turbulent flat plate at M_∞= 2.0 and Re_∞ = 3.762E06.

4 Conclusions

A numerical solver based on the collisional BGK model of the Boltzmann equation has been successfully developed to simulate two-dimensional compressible turbulent flow based on the Reynolds-Averaged Navier-Stokes equations which utilizes a combined k-ε / k-ω SST turbulence model to provide the turbulent eddy viscosity. A supersonic flow over a flat plate which undergoes transition from laminar to turbulent flow is selected in the current study to asses the numerical capabilities of this solver. The computed results for this test case clearly demonstrate that the BGK scheme is able to provide a good resolution of the flow. This claim is justified by comparisons of the numerical findings of the BGK scheme with existing analytical data and numerical results from other renowned numerical solvers.

5 Acknowledgement

The authors would like to acknowledge the support of the Ministry of Science, Technology and Innovation, Malaysia under the grant No. 09-02-08-10004-EAR.

6 References

[1] Spalding, D.B. and Chi, S.W., "The drag of a compressible turbulent boundary layer on a smooth plate with and without heat transfer," J. of Fluid Mechanics, Vol. 18, No. 1, pp 117-143, 1964.

[2] Hoffmann, K.A.; and Dietiker, J.F.; "Student Guide to CFD," Engineering Education System, Wichita, Kansas, vol. 3, chap. 21, 2001.

[3] Ong, J.C.; Omar, A.A.; Asrar, W.; and Hamdan, M.M.; "Development of Gas-Kinetic BGK Scheme for Two-Dimensional Compressible Inviscid Flows," AIAA Paper 2004-2708, 2004.

[4] Xu, K.; "Gas-Kinetic Theory Based Flux Splitting Method for Ideal Magnetohydrodynamics," ICASE Report, 98-53, Nov. 1998.

[5] Chae, D.S.; Kim, C.A.; and Rho, O.H.; "Development of an Improved Gas-Kinetic BGK Scheme for Inviscid and Viscous Flows," Journal of Computational Physics, vol. 158, pp. 1-27, 2000.

[6] Ong, J.C.; Omar, A.A.; and Asrar, W.; "Evaluation of Gas-Kinetic Schemes for 1D Inviscid Compressible Flow Problem," International Journal of Computational Engineering Science (IJCES), vol. 4, no. 1, pp. 829-851, Dec. 2003.

[7] Ong, J.C.; Omar, A.A.; Asrar, W.; and Hamdan, M. M.; "An Implicit Gas-Kinetic BGK Scheme for Two-Dimensional Compressible Inviscid Flows," AIAA Journal, vol. 42, no. 7, pp 1293-1301, 2004.

[8] Ong, J.C.; Omar, A.A.; Asrar W.; and Zaludin, Z.A.; "Gas-Kinetic BGK Scheme for Hypersonic Flow Simulation," AIAA Paper, 2006-0990, Jan. 2006.

[9] Addusslam, S.N.; Ong, J.C.; Harun, M.M.; Omar, A.A.; and Asrar, W.; "Application of Gas-Kinetic BGK Scheme for Solving 2-D Compressible Inviscid Flow around Linear Turbine Cascade," Int. Journal for Computational Methods in Engineering Science and Mechanics, vol. 7, no. 6, Nov. 2006.

[10] Leonard, A.; "Energy Cascade in Large-Eddy Simulations of Turbulent Fluid Flows," Advances in Geophysics, vol. 18A, pp. 237-248, 1974.

[11] Liu, Z.; Zhao, W.; and Liu, C.; "Direct Numerical Simulation of Transition in a Subsonic Airfoil Boundary Layer," AIAA-97-0752, January, 1997.

[12] Hatay, F.F.; and Biringen, S.; "Direct Numerical Simulation of Low-Reynolds Number Supersonic Turbulent Boundary Layers," AIAA-95-0581, January, 1995.

[13] Ng, K.C.; Yusoff, M.Z.; and Yusaf, T.F.; "Simulations of Two-Dimensional High Speed Turbulent Compressible Flow in a Diffuser and a Nozzle Blade Cascade," American Journal of Applied Sciences 2 (9), pp. 1325-1330, 2005.

[14] Georgiadis, N.J.; Drummond, J.E.; and Leonard, B.P.; "Evaluation of Turbulence Models in the PARC Code for Transonic Diffuser Flows," AIAA-94-0582, January, 1994.

[15] Xu, K.; "Gas-Kinetic Scheme for Unsteady Compressible Flow Simulations," Von Kármán Ins. for Fluid Dynamics Lecture Series, vol. 1998-03, *Von Kármán Ins., Rhode St. Genese, Belgium,* 1998.

[16] Hoffmann, K.A.; and Chiang, S.T.; "Computational Fluid Dynamics for Engineers," Engineering Education System, Wichita, vol. 2, chap. 11 and 14, 1993.

[17] Hoffmann, K.A.; and Chiang, S.T.; "Computational Fluid Dynamics for Engineers," Engineering Education System, Wichita, vol. 3, chap. 21, 2000.

[18] Hirsch, C.; "The Numerical Computation of Internal and External Flows," John Wiley & Sons, New York, vol. 2, chap. 21, 1990.

[19] Ong, J.C.; "Computational Analysis of Gas-Kinetic BGK Scheme for Inviscid Compressible Flow," M. Sc. Thesis, University Putra Malaysia, Malaysia, 2004.